SANDIA REPORT

SAND2017-13566
Unlimited Release
Printed December 2017

Feasibility Study for a Combined Radiation Environment in the ACRR-FRECII Cavity

Edward J. Parma

Prepared by
Sandia National Laboratories
Albuquerque, New Mexico 87185 and Livermore, California 94550

Sandia National Laboratories is a multimission laboratory managed and operated by National Technology and Engineering Solutions of Sandia LLC, a wholly owned subsidiary of Honeywell International Inc. for the U.S. Department of Energy's National Nuclear Security Administration under contract DE-NA0003525.

Issued by Sandia National Laboratories, operated for the United States Department of Energy by Sandia Corporation.

Available to DOE and DOE contractors from
U.S. Department of Energy
Office of Scientific and Technical Information
P.O. Box 62
Oak Ridge, TN 37831

Telephone: (865) 576-8401
Facsimile: (865) 576-5728
E-Mail: reports@adonis.osti.gov
Online ordering: http://www.osti.gov/bridge

Available to the public from
U.S. Department of Commerce
National Technical Information Service
5285 Port Royal Rd.
Springfield, VA 22161

Telephone: (800) 553-6847
Facsimile: (703) 605-6900
E-Mail: orders@ntis.fedworld.gov
Online order: http://www.ntis.gov/help/ordermethods.asp?loc=7-4-0#online

SAND2017-13566
Unlimited Release
Printed December 2017

Feasibility Study for a Combined Radiation Environment in the ACRR-FRECII Cavity

Edward J. Parma
Sandia National Laboratories
P.O. Box 5800
Albuquerque, NM 87185

Abstract

The objective of this report is to determine the feasibility of a combined pulsed-power accelerator machine, similar to HERMES-III, with the Annular Core Research Reactor (ACRR) Fueled-Ring External Cavity (FREC-II) in a new facility. The document is conceptual in nature, and includes some neutronic analysis that illustrates that that the physics of such a concept would be feasible. There would still be many engineering design considerations and issues that would need to be investigated in order to determine the true viability of such a concept. This report does not address engineering design details, the cost of such a facility, or what would be required to develop the safety authorization of the concept.

The radiation requirements for the "on-target" gamma-ray dose and dose rate are not addressed in this report. It is assumed that if the same general on-target specifications for a HERMES-III type machine could be met with the proposed concept, that the machine would be considered highly useful as a radiation effects sciences platform.

In general, the combined accelerator/ACRR reactor concept can be shown to be feasible with no major issues that would preclude the usefulness of such a facility. The new facility would provide a capability that currently does not exist in the radiation testing complex.

Acknowledgements

The author wishes to thank Pat Griffin and Ken Reil for their valuable input, and Curtis Peters for his assistance in building the models and running MCNP.

Contents

Figures

1. Introduction

The objective of this report is to determine the feasibility of a combined pulsed-power accelerator machine, similar to HERMES-III, with the Annular Core Research Reactor (ACRR) Fueled-Ring External Cavity (FREC-II) in a new facility. The document is conceptual in nature, and includes some neutronic analysis that illustrates that that the physics of such a concept would be feasible. There would still be many engineering design considerations and issues that would need to be investigated in order to determine the true viability of such a concept. This report does not address engineering design details, the cost of such a facility, or what would be required to develop the safety authorization of the concept.

The radiation requirements for the "on-target" gamma-ray dose and dose rate are not addressed in this report. It is assumed that if the same general on-target specifications for a HERMES-III type machine could be met with the proposed concept, that the machine would be considered highly useful as a radiation effects sciences platform.

Could a pulsed-power accelerator be joined to the ACRR to form a unique combined environment facility? This concept would not be feasible using the current ACRR facility. There are simply no infrastructure capabilities at the current facility to allow accommodation and integration of this type of machine with the ACRR. A new facility is required that would integrate a pulsed-power facility with a new ACRR facility. The size of the pulsed-power facility would be dependent on the desired output of the machine in a standalone mode and in combination with the ACRR. Since the HERMES-III machine is considered the gold standard for radiation dose rate and total dose on target, one would want to determine if the same type of machine could be integrated with the ACRR.

In considering the integration with the ACRR, it is assumed that the gamma-ray source-target region would be in an ACRR cavity at the axial centerline of the core, to allow efficient coupling with an experiment being fielded in the ACRR or FREC-II cavity. However, in consideration of the geometry of ACRR, there would simply be no feasible way to integrate a pulsed-power machine's vacuum-jacketed magnetically-insulated transmission line (MITL) into the central cavity of the ACRR. This is because it is impossible to remove ACRR fuel elements and maintain the operational conditions of the reactor. The only way this could be accommodated would be to have a MITL enter the cavity from below or above the reactor tank. This would be difficult if not impossible to configure.

A more feasible integration concept would be to have a MITL that penetrated the ACRR tank from the side and into or near the FREC-II cavity. Having the MITL enter the FREC-II from the backside of the FREC-II would be preferable, to limit the asymmetric neutron fluence on an experiment package. MCNP neutronic results presented in this report show that the penalty for this type of configuration is not a huge disadvantage, as compared to the current FREC-II cavity neutron fluence.

2. ACRR-FREC-II Description

The ACRR facility is located in TA-V at Sandia National Laboratories in Albuquerque, NM. The ACRR has been operational in its current fueled configuration since 1977. In 1988, the FREC-II became operational using the previous ACPR UZrH fuel. The specifications and operating conditions for the ACRR and FREC-II can be found in the published radiation characterization summary documents. [1-2] The ACRR is a pool-type pulse reactor. The customer base for the ACRR has historically been derived from the pulsing capabilities of the reactor. There are three unique characteristics of the ACRR that make it one of the most useful neutron/gamma-ray pulse radiation test facilities in the world. Firstly, the ACRR fuel is a unique UO_2-BeO form that allows for a high heat capacity and pulsing capabilities over three times that which can be achieved in any pulse TRIGA reactor. Secondly, the ACRR central cavity is a 9-inch dry cavity which passes directly through the center of the core. Thirdly, the ACRR maintains a fast/epithermal neutron spectrum in the cavity which allows for the neutron spectrum to be modified using "buckets." Since the ACRR is almost exclusively used for its pulsing capabilities, the fuel has very little burnup and is the same fuel that was originally fueled in the core in 1977. It is expected that at the continued operational level, the core will last many more decades.

The FREC-II maintains a 20-inch dry cavity that allows for larger experiments to be fielded. The FREC-II can be connected (coupled) to the ACRR or tilted back (decoupled). In the coupled mode, the FREC-II maintains poison-element FREC rods that can be inserted or removed from the back region of FREC-II to allow for flux tilting in the 20-inch cavity. With the FREC-II decoupled from the ACRR, the ACRR behaves as though it were a standalone reactor. The FREC-II offers some attributes that experimenters may desire. The larger cavity allows for larger experiments to be fielded in the reactor. The FREC rods allow for the flux shape to be changed in the cavity. A maximum pulse can be performed with a lower total neutron fluence in the FREC-II, as compared to the ACRR cavity, allowing for shorter pulse widths for an active-type experiment.

Figure 1 shows the ACRR and FREC-II operating at a steady-state power in the coupled mode. Figure 2 shows a 3-D image of the ACRR tank and an enlarged image of the ACRR with FREC-II in the decoupled mode.

- 236 UO_2-BeO fueled elements
  1.5 in (3.8 cm) dia. x 20 in (51 cm)
  100 g U-235 per element – 35% enr.
- Operating Power level
  4 MW_{th} Steady State Mode
  250 MJ Pulse Mode (6 ms FWHM)
  300 MJ Transient Mode (Programmable)
- Dry cavity 9 in (23 cm) diameter
  Extends full length of pool through core
  Neutron Flux 4E13 n/cm²-s at 2 MW
  65% > 1 eV, 56% > 10 keV, 45% > 100 keV
- Epithermal Spectrum
  Flux in cavity can be tailored for desired energy spectrum (Poly, B4C)
- Open-pool type reactor
  Fuel elements cooled by natural convection
  Pool cooled by HX and cooling tower
- FREC-II uses previous ACPR fuel
  TRIGA type (UZrH) – 20 in (51 cm) dia. dry cavity
- Fuel burnup is minimal
  Reactor used for short duration power runs, pulses, and transients

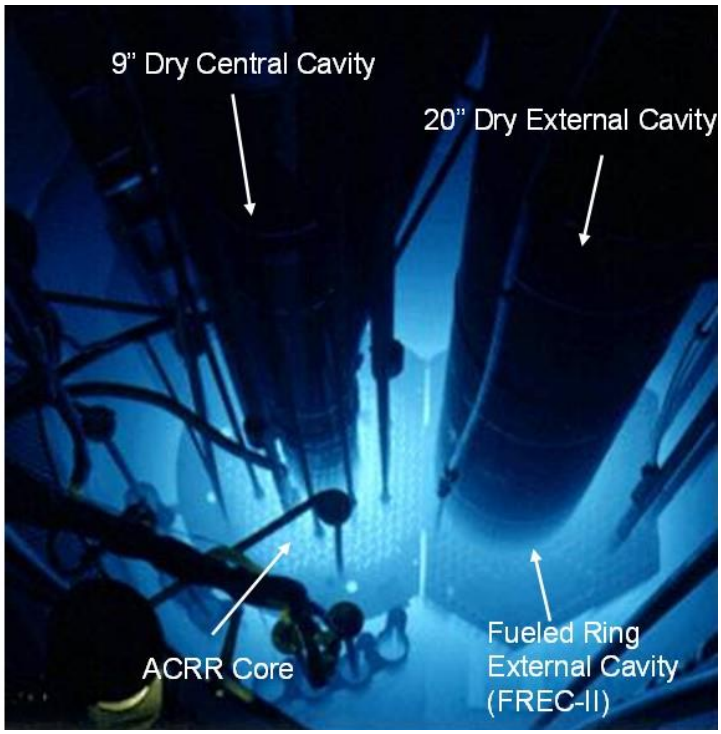

Figure 1. The ACRR and FREC-II Operating in the Coupled Mode.

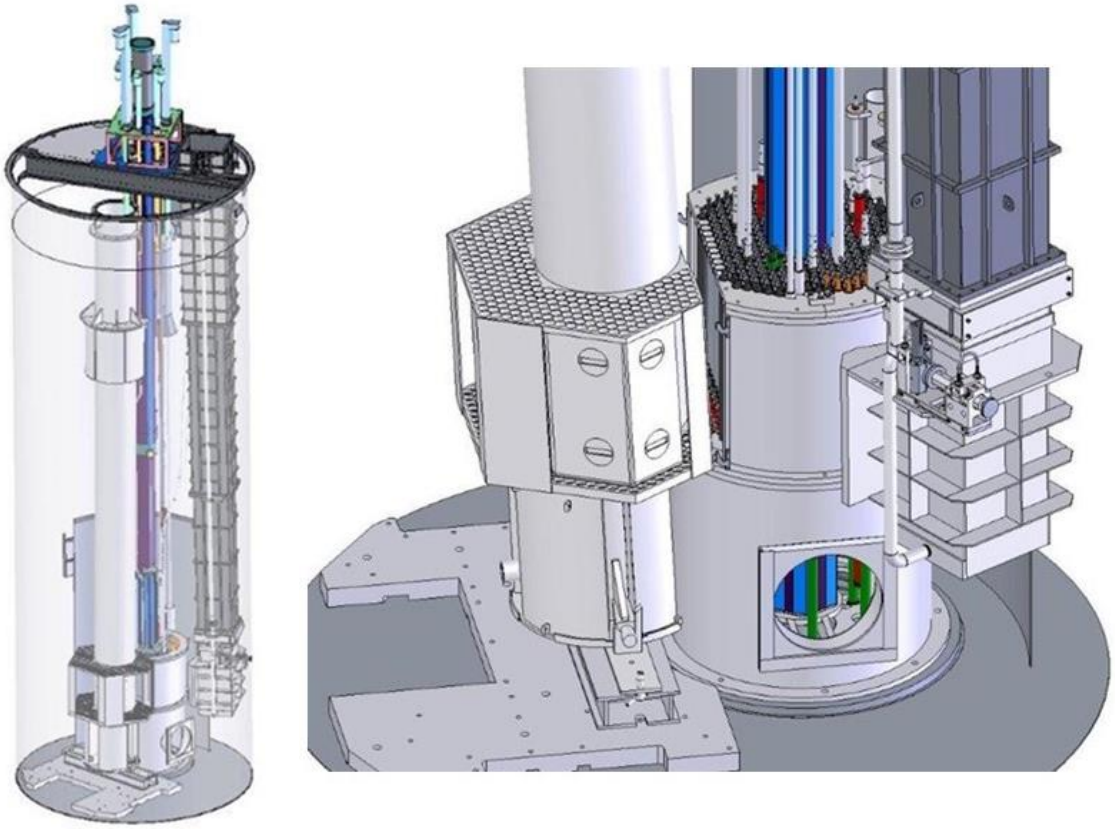

Figure 2. Image of the ACRR Tank, ACRR, and FREC-II in the Decoupled Mode.

Extensive neutronic modeling of the ACRR/FREC-II has been performed using the Monte-Carlo code MCNP. Shown in Figure 3 is the MCNP model with the FREC-II coupled. Shown are the three void chambers associated with FREC-II. The purpose of these chambers is to direct neutrons towards the rear of the FREC-II in order to achieve a more uniform spatial neutron flux in the FREC-II cavity. The void chambers are sealed aluminum cans that extend from the lower grid plate to the upper grid plate. The limited amount of ZrH fuel available constrained the size and configuration for the FREC-II geometry. In total, 186 elements, including the four FREC rods, are available and are used in FREC-II. Also, shown in Figure 3 are the four FREC rods. These rods are B_4C poison elements that are fuel followed, and are used to geometrically shape the neutron flux in the FREC-II cavity. The FREC-II can be operated with the FREC rods full in, full out, or at any position in between. See reference [2] for more information on flux shape and tilting capabilities using the FREC rods. Readily seen in the MCNP model is the rear void chamber of FREC-II. Since there are not many fuel elements in this region of FREC-II, it is envisioned that a MITL port, with a vacuum jacketed MITL from a pulse-power accelerator, could be incorporated into this region of FREC-II. This would allow for direct exposure of an experiment in the FREC-II cavity with a high gamma-ray radiation dose prior to, or after a reactor pulse.

Figure 4 shows one of the conceptual MCNP models analyzed, illustrating how a MITL port could be designed to interface with the FREC-II. Several concepts will be analyzed and compared to the baseline ACRR-FREC-II model later in this report.

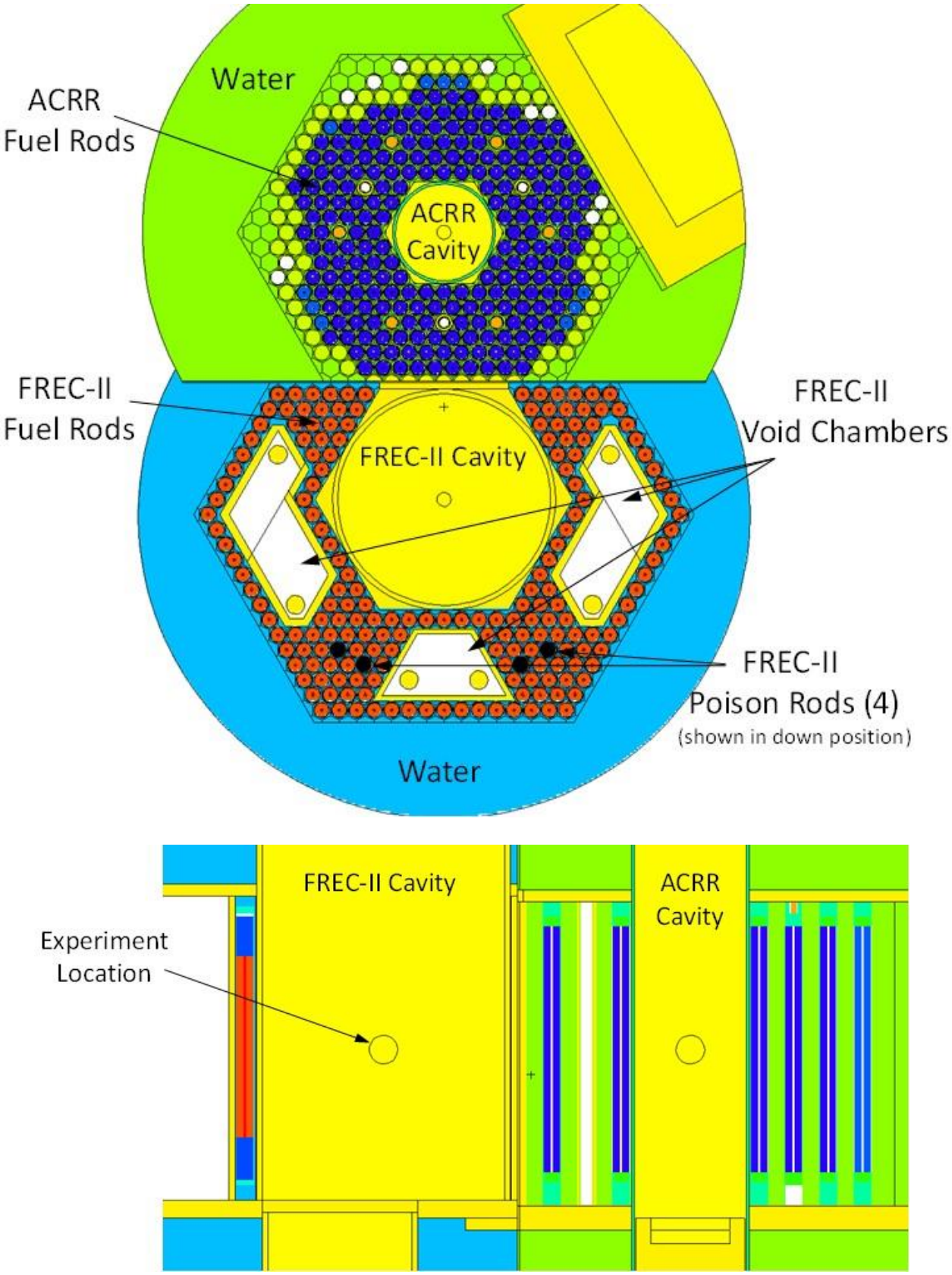

Figure 3. MCNP Model of the ACRR and FREC-II Coupled.

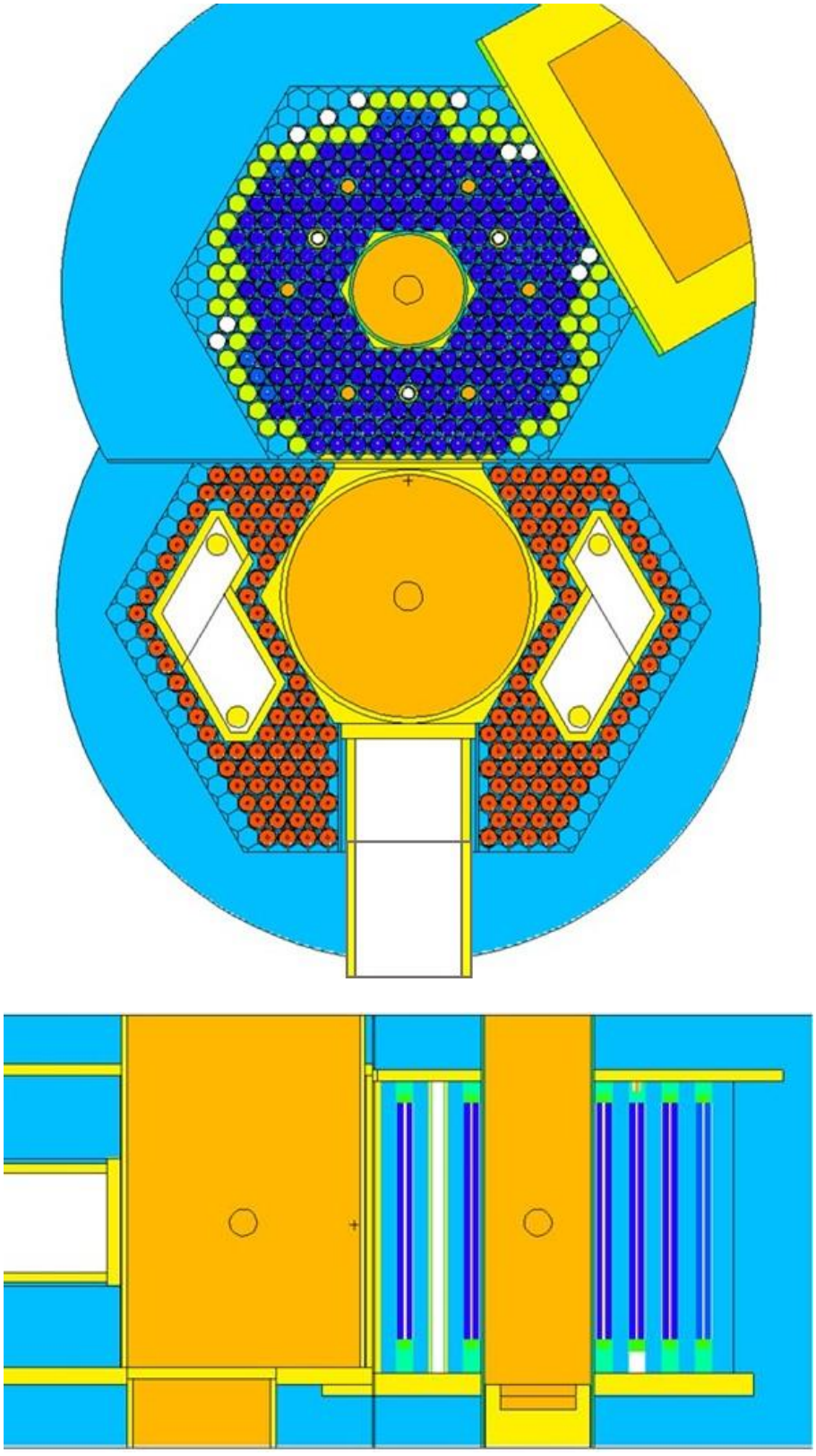

Figure 4. MCNP Model of the Modified FREC-II Coupled to the ACRR – 10.2 in. Diameter MITL Port.

3. HERMES-III Description

The High-Energy Radiation Megavolt Electron Source (HERMES-III) accelerator is the world's most powerful gamma-ray simulator, primarily used to demonstrate the rate effects of gamma-ray radiation on materials, electronic components, and electronic devices. HERMES-III has both indoor and outdoor test cells and is used predominantly for simulating the effects of prompt radiation from a nuclear burst on electronics and complete military systems. It can produce eight shots per day, four days a week. HERMES-III can produce 13 TW of power in a 19-MeV, 700-kA, 28-ns electron beam. This allows for a dose on target of 100 krad (Si) in 20 ns or 5e12 rad(Si) per second. It uses technology developed by Pulse Sciences, Inc, and SNL in the joint Defense Special Weapons Agency/DOE Linear Induction Accelerator Program. HERMES-III is located in TA-IV. The first fully integrated shots were performed in 1988.

The accelerator subsystems consist of ten Marx generators, twenty intermediate energy store capacitors, twenty 2.2-uV laser-triggered gas switches, eighty 1.1-MV pulse-forming transmission lines (PFLs), and twenty inductively isolated cavities that deliver the energy to a magnetically insulated transmission line (MITL) adder network. An extension MITL delivers the output from the adder to an indented-anode electron beam diode/converter. Current flows down the MITL to the anode target. Gamma rays are generated as Bremsstrahlung as the electrons slowdown in the high Z target, such as tantalum. The target materials must have enough heat capacity to prohibit melting and vaporization as the energy is deposited over a short range.

Figures 5 and 6 show an artist's rendering of the HERMES-III machine and an overall picture of the facility, respectively. The HERMES-III MITL is 50 feet in length. The overall width of HERMES-III is 80 feet. The diameter of the MITL on target is somewhat variable. Typically, the target diameter is about 20 inches. A smaller diameter target is achievable at the expense of having a higher energy density and the potential for melting or vaporization of the target materials.

Some of the important features of HERMES-III include the following:

- 20 cavities;
- 80 PFLs, 5 ohm, 40 ns;
- 1.0-MV cavity voltage;
- 20 MV output voltage;
- 0.7 MA current;
- 50 ft MITL;
- 80 ft dia. versus 10 ft LTD;
- 100 krad (Si) in 20 ns => 5e12 rad(Si)/sec.

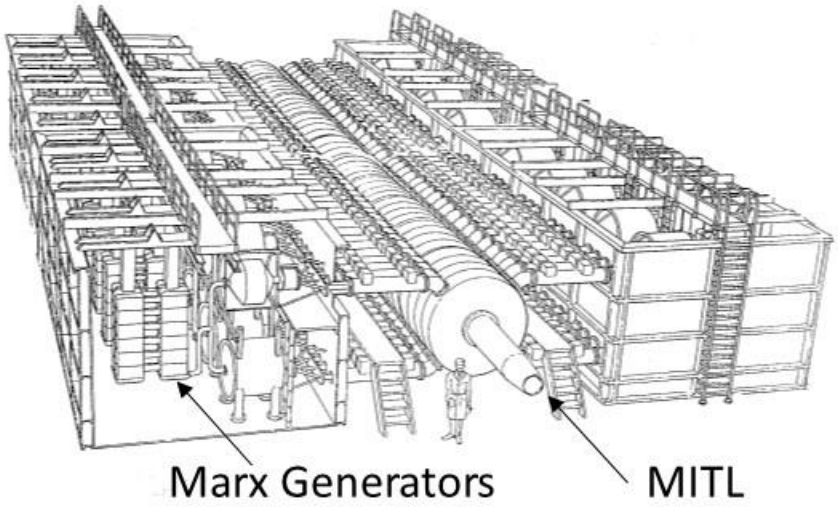

Figure 5. Artist's Depiction of the HERMES-III.

Figure 6. The HERMES-III Facility.

4. Proposed New Facility Description

The proposed new facility is shown conceptually in Figures 7-9. Figure 7 shows an elevation view of the facility. Figures 8 and 9 show plan views for two options, a straight MITL and a curved MITL, respectively, from the accelerator into the ACRR tank and the FREC-II cavity. A curved MITL may be required to minimize the radiation streaming from the reactor back through the accelerator during combined tests. Radiation streaming will not be analyzed in this report but would be required in a feasibility analysis.

The ACRR portion of the facility could be approximately the same size as the current facility, about 50 ft x 80 ft with a high bay of ~ 30 ft. The top of the reactor tank would be near ground level and be about 30 ft deep. The accelerator facility would be required to be below grade (~30 ft), in order to maintain a level MITL into the ACRR tank and into the FRECII. The facility would be at least 100 ft x 100 ft with a high bay. The accelerator could be on a railroad-type track to allow it to be positioned away from the ACRR for standalone operations and maintenance. A coupling MITL port into the ACRR tank would allow for the portion of the MITL that is near the ACRR to be removed, allowing for a shorter MITL and securing of activated components. In the standalone mode, the accelerator could continue to be used with experimental setup in the test cell area. Additional shielding could be placed in the MITL port and in the test cell to minimized the radiation dose levels in the test cell during reactor operations. The MITL port and test cell could also be set up for performing neutron radiography, when the accelerator MITL is removed.

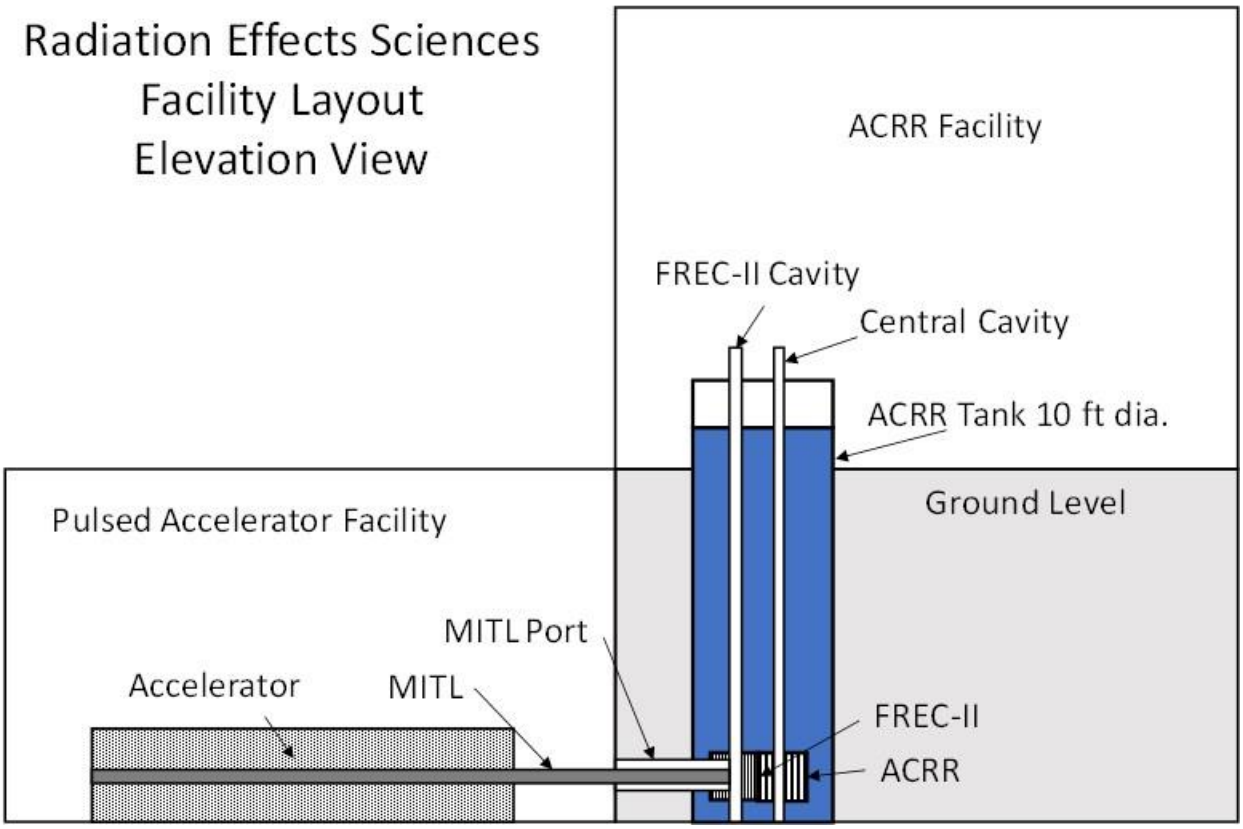

Figure 7. Conceptual Plan View of the ACRR Combined Facility.

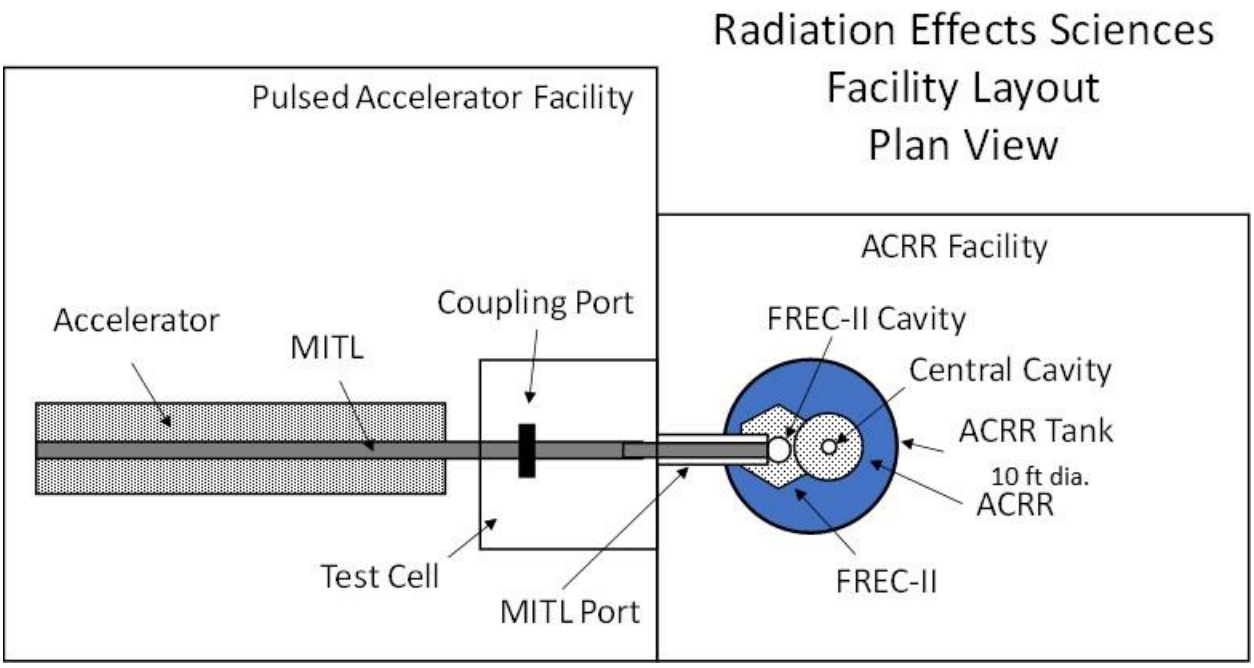

Figure 8. Conceptual Elevation View of the ACRR Combined Facility With Straight MITL.

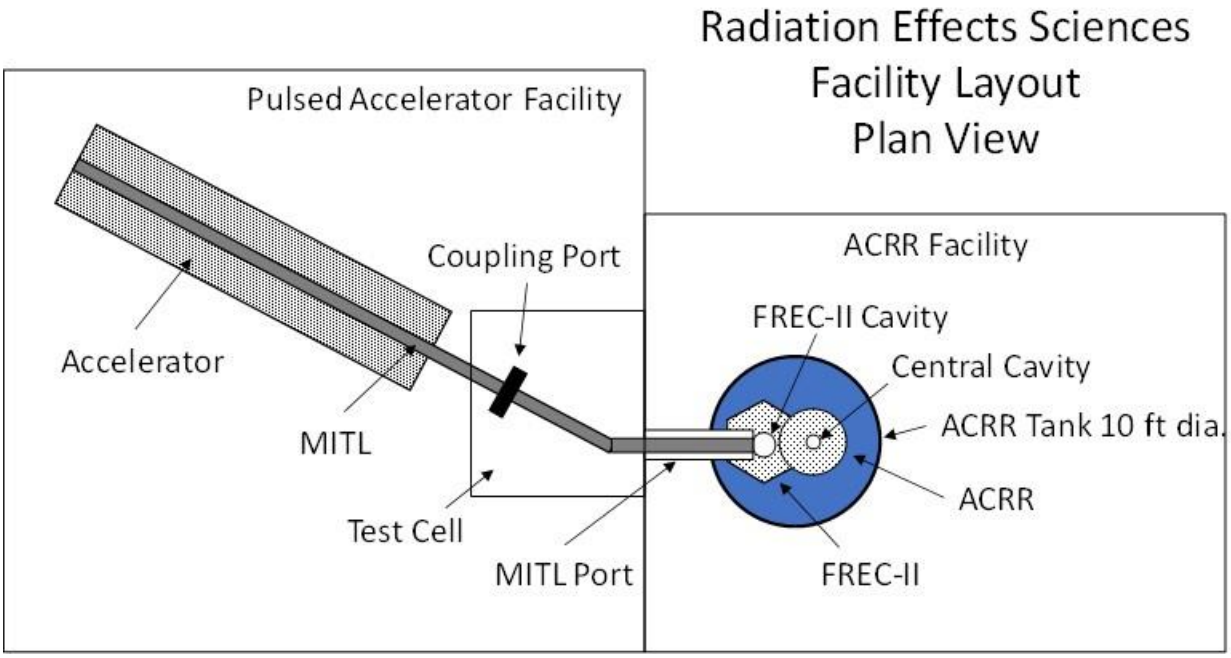

Figure 9. Conceptual Elevation View of the ACRR Combined Facility With Curved MITL.

5. Integration of the Accelerator MITL With the ACRR-FREC-II

Figure 3 shows the MCNP model for the ACRR with FRECII coupled. The most logical location to include a MITL into the ACRR would be through the back of FREC-II. In that region, there is only a small amount of fuel that would be required to be displaced. Figure 4 shows one option that was analyzed with a 10.2 diameter MITL port. In this option, 22 fuel elements were removed from the rear portion of FREC-II along with the rear void chamber. A voided cylinder, fabricated from aluminum, 10.2 in. in external diameter was placed at the fuel axial centerline.

The MITL, converter, and target are shown conceptually in Figure 10. The MITL for a linear accelerator is made up of two concentric tapered tubes. The outer tube is the anode, is grounded, and maintains a vacuum internally. The inner tube is the cathode and conducts the electrons down the conductor. The magnetic field that is induced by the pulsed current flow forces the electrons to remain on the cathode and travel down the cathode during the pulse. Both tubes are closed at the end but do not touch. The inner tube conducts the electrons to the end of the tube, where the electrons strike the bremsstrahlung converter plate, which is part of the anode. The converter plate is typically a thin, high Z material such as tantalum. As the electrons slowdown in the converter plate, Bremsstrahlung radiation (gamma rays and x-rays) are emitted from the plate. The converter plate is typically 120 mils (3 mm) in thickness and is backed by graphite and other heat absorbing materials. Melting and vaporization of the converter plate can occur if the energy density is too high. At HERMES-III, the end of the MITL is ~15 in. diameter. Its diameter is a parameter that can be varied depending on the energy density desired and the desired uniformity of the photon fluence.

The MITL would be interfaced with the ACRR through the MITL port that would be a permanent part of the ACRR tank. As shown in Figure 11, the port would extend from outside of the tank to within the tank to a position congruent with the positioning of the FREC-II location and would be welded in place to form a structurally sound water tight seal. The ACRR tank, as it currently exists, is ¼ in. thick stainless steel. The tank at the new facility would most likely be designed and fabricated in a similar manner. A MITL extension, that would include the Bremsstrahlung converter, would be a removable feature that would fit within the port. The port could be sealed off when not in use, and flooded or filled with neutron and gamma-ray shielding materials, to minimize the dose levels in the test cell, when the MITL was not being used.

Defining how the ACRR, FREC-II, and MITL port would all interface and operate together in a new facility is an important consideration. Currently, as shown in Figure 2, the FREC-II is tilted back several degrees from its base when the ACRR is operated in the uncoupled mode. In this mode, a nickel plate is inserted at the FREC interface on the ACRR, allowing for a nickel reflector around the perimeter of the ACRR core. The simplest approach for a new facility would be to use the same basic principle of tilting the FREC-II. However, this would mean that the MITL port would not be able to be directly in contact with the FREC-II cavity. This could still allow for the on-target dose rate requirements to be achieved, but would need to be investigated further.

Another approach would be to have the FREC-II position fixed in place and move the ACRR core, control rods, and control rod drives laterally on a track to mate with the FREC-II, when desired. Another approach would be to have a retractable portion of the MITL port, which O-rings to maintain water tightness. This approach could complicate the safety review process, considering that the O-rings could leak or fail.

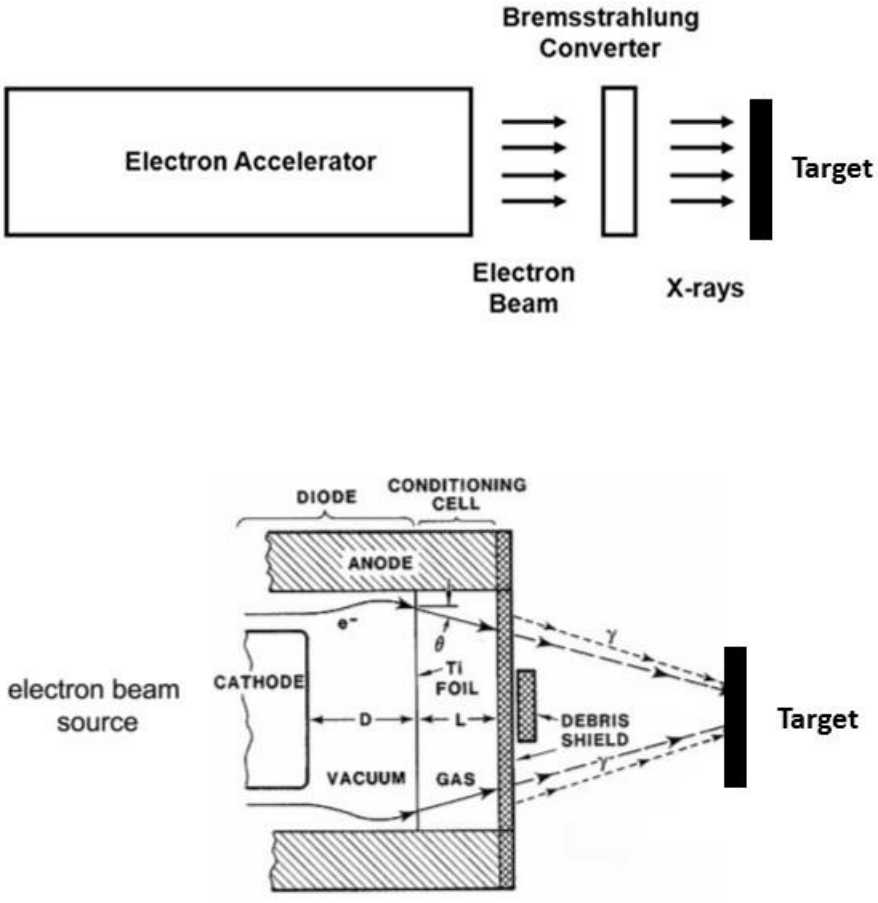

Figure 10. Conceptual View of the MITL, Converter, and Target.

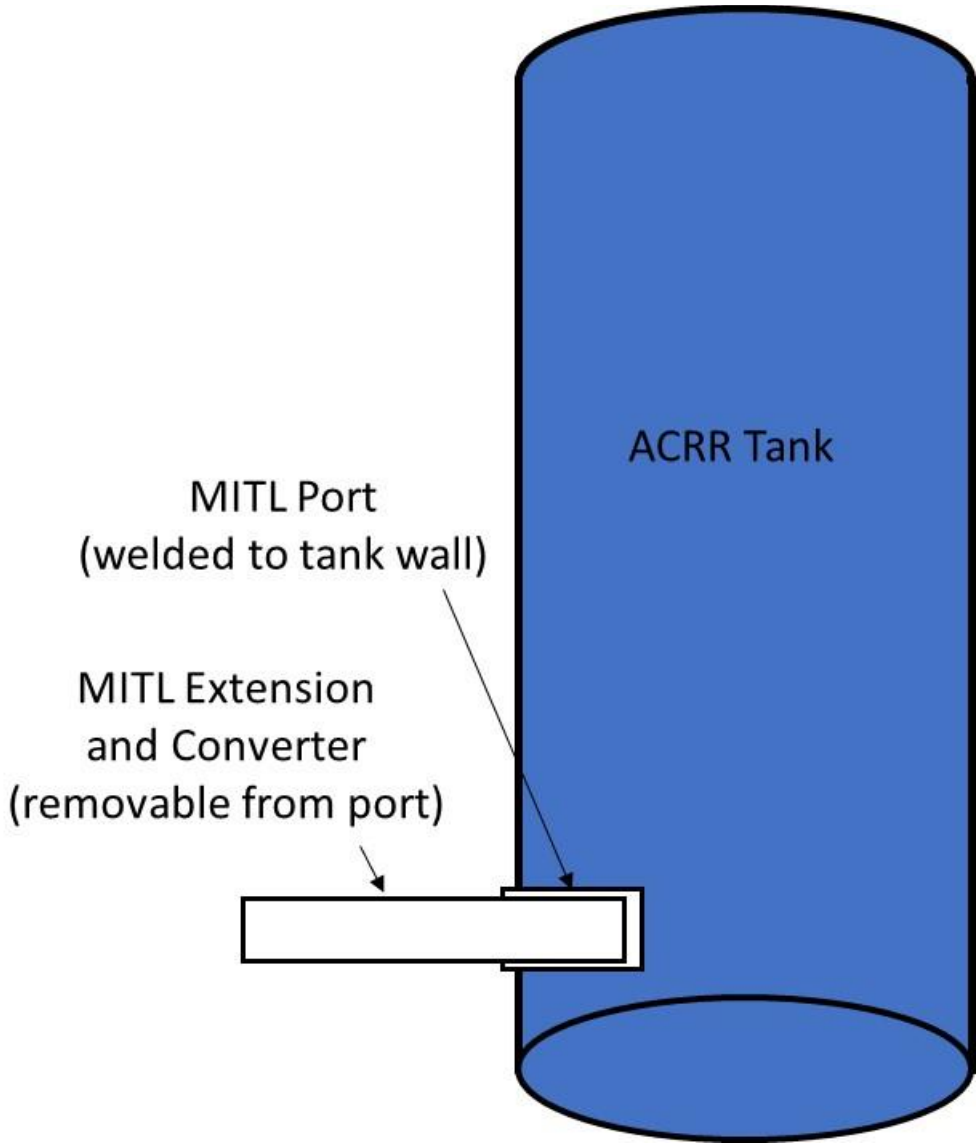

Figure 11. Conceptual View of the ACRR Tank with MITL Port and Extension.

6. Proposed Accelerator Design

Although a HERMES-III type machine could be built and integrated at the new facility, a more modern accelerator design, using Linear Transformer Driver (LTD) architecture, would be better suited for this type of facility. The LTD architecture is discussed in more detail in Appendix A of this report. Sandia continues to develop this technology. This technological approach can provide very compact devices that can deliver very fast, high-current and high-voltage pulses. The footprint of these types of machines, as compared with current-day pulsed-power accelerators, is considerably smaller since LTDs do not require large oil and deionized water tanks. This makes them ideally suited for applications that require portability and size constraints. A LTD accelerator would be the most compact design strategy, if it can be shown to deliver the dose and dose rate metrics desired on target. The LTD concept could be more compactly designed to fit on a railroad-type track and be moved within the facility.

7. Neutronic Models and MCNP Analyses

The neutronics code MCNP has been used extensively to model the neutron and gamma-ray transport in the ACRR and FREC-II. To determine the neutronic effects that a MITL port would have on the operation of the FREC-II and the neutron and gamma-ray response in the FREC-II cavity, several model permutations of ACRR/FREC-II were analyzed.

The standard geometry with FREC-II coupled to the ACRR is shown in Figure 3. The sphere at the center of the FREC-II cavity represents a tally scoring sphere where an experiment could be located. Metrics can be tallied at this location using MCNP to determine differences from permutations removing fuel from the rear of FREC-II and adding a MITL port. Three permutations were considered in this analysis. Figure 4 shows the model with a 10.2 in. diameter MITL port, Figure 12 with a 11.9 in. diameter MITL port, and Figure 13 with a 10.2 in. diameter MITL port with all the FREC fuel removed. The last case represents a condition for academic purposes, if all the FREC fuel were removed from the FREC-II.

For all the cases, the MITL port was an aluminum tube 2 cm in thickness. The sizes are such that the four FREC rods, seen in Figure 3, can remain in place. No other geometry changes were made, except for removing fuel and the rear void chamber. For the 10.2 in. diameter port, 22 FREC fuel elements were removed from the 186 total. For the 11.9 in. diameter port, 30 FREC fuel elements were removed from the 186 total.

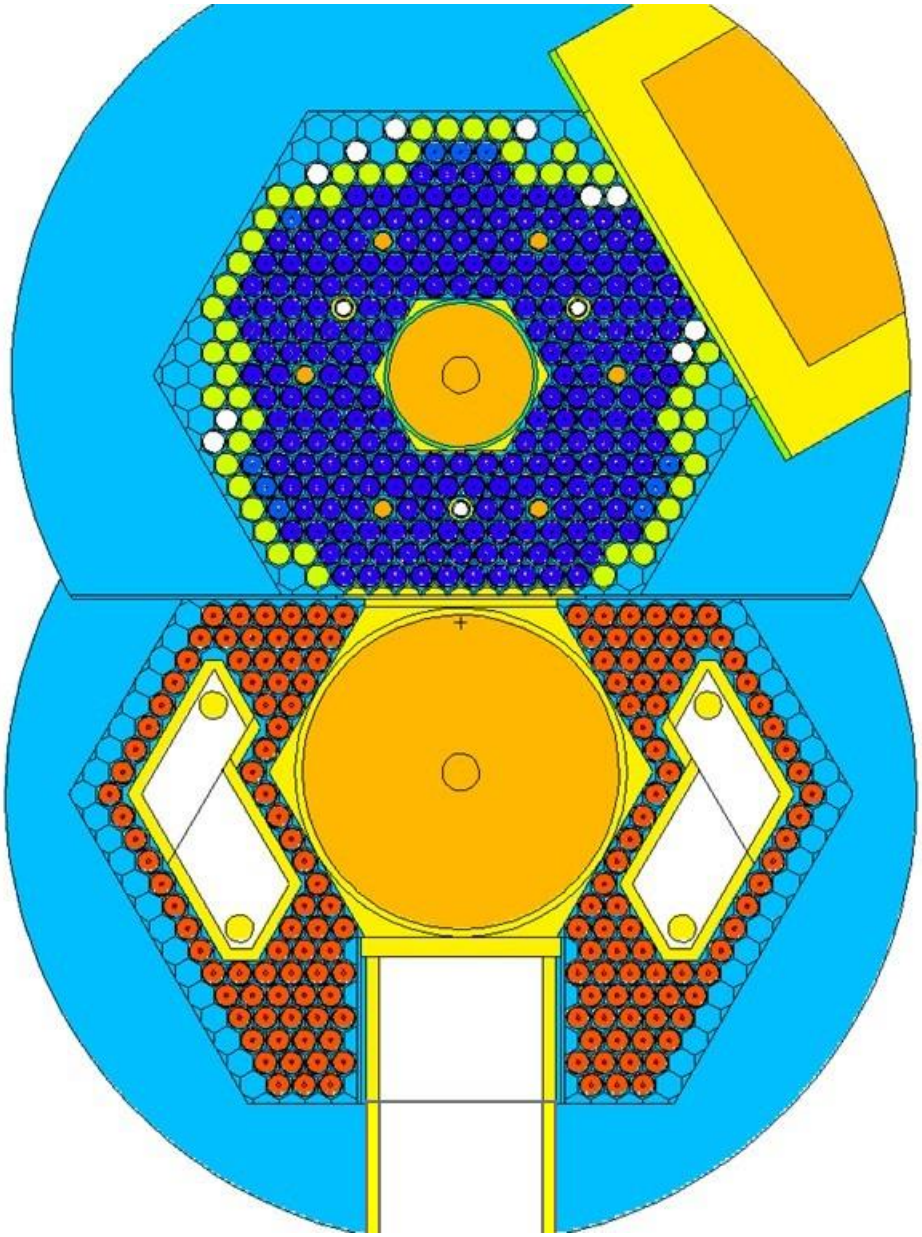

Figure 12. MCNP Model of the Modified FREC-II Coupled to the ACRR – 11.9 in. Diameter MITL Port.

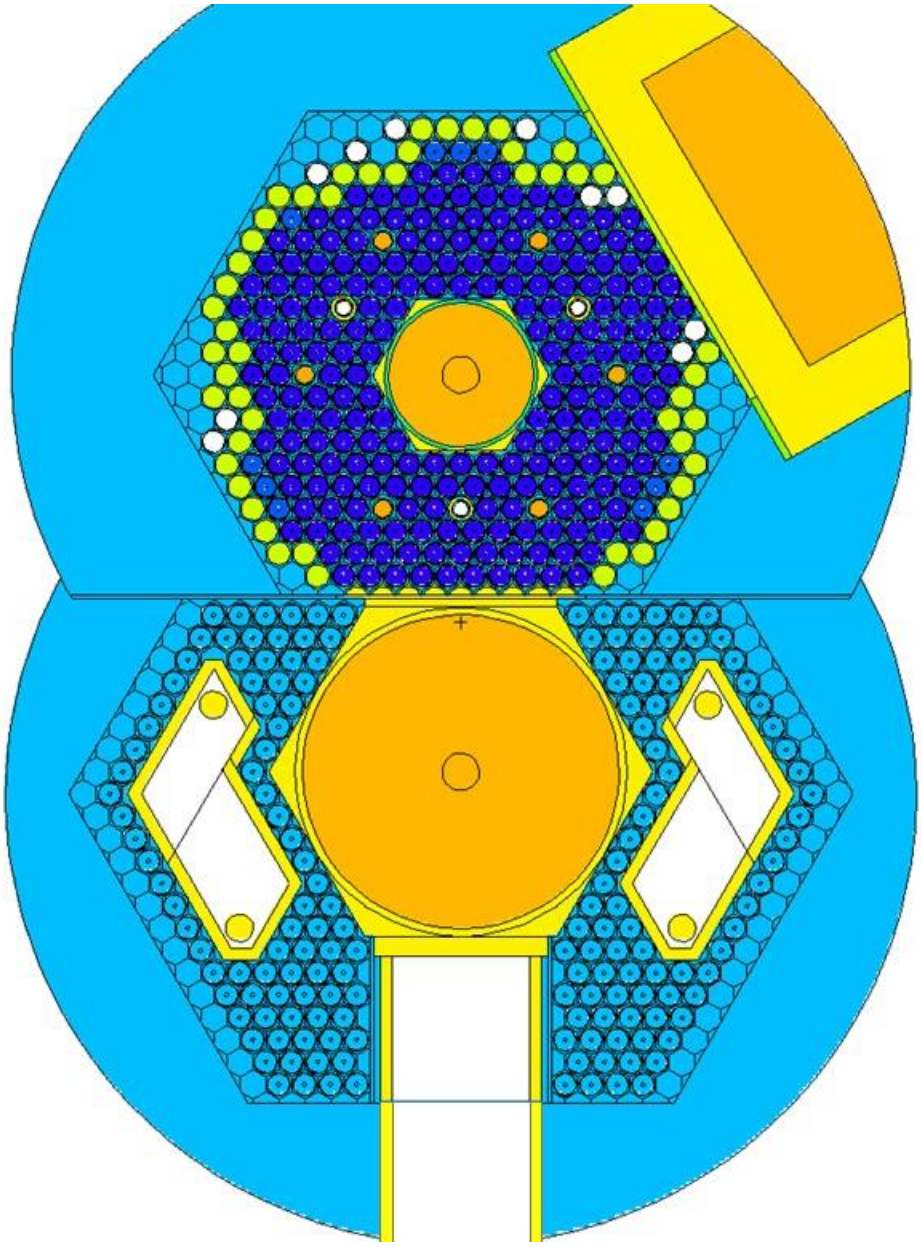

Figure 13. MCNP Model of the Modified FREC-II Coupled to the ACRR – 10.2 in. Diameter MITL Port With all FREC Fuel Removed.

Table 1 shows some of the important metrics calculated in MCNP at the tally sphere in the FREC-II cavity for the default condition (nominal FREC-II case with the FREC rods up and down), with the 11.9 in. MITL port (FREC rods up and down), and for the 10.2 in. MITL (FREC rods up and the no-fuel condition). Calculated metrics include the value for keff and the change in reactivity, the neutron lifetime, the total neutron fluence, the 1-MeV damage equivalent in silicon (DES) neutron fluence, and the prompt gamma-ray ionizing dose. For all of the geometry cases analyzed, the MCNP model was set such that the FREC rods were either full up or full down, the ACRR safety elements (2) were full out, the ACRR transient rods (3 not fuel followed) were full out, and the control rod bank (6) were positioned such that keff would be near 1.025 (~$3.50) for the nominal FREC-II case with the FREC rods up. The position of the ACRR elements was maintained for all of the other cases analyzed. This condition would allow for a direct comparison of the results. A positive reactivity condition of $3.50 corresponds to a maximum pulse in the ACRR. The MCNP runs were all performed with the cross sections at 300K.

The results were compared to determine significant differences in the metrics for the different geometries analyzed. Comparing reactivity differences between the cases, it is seen that there is only a few cents difference between these results with the FREC-II case with the FREC rods down. The major difference is between the nominal FREC-II case with the FREC rods up compared to the FREC rods down, and compared to the case with no fuel in FREC-II. But even for this case, the difference in reactivity is only $0.25, which is a small value.

The neutron lifetime has a direct effect on the pulse width. For ACRR with FREC-II in the decoupled mode, the neutron lifetime is about 24 μsec. Notice that for all of the case except for the nominal FREC-II case with the FREC rods up, the neutron lifetime is very close to this value. For the nominal case with the FREC rods up, the neutron lifetime is about 27 μsec. Pulse widths for the FREC rods up are always slightly larger than for the FREC rods down. This implies that, with a MITL port in place, the reactor will behave very similarly to the nominal FREC-II case with the FREC rods down, for pulse conditions.

The radiation exposure metrics show similar comparative results to the nominal FREC-II case with the FREC-II rods down. The values are within 10% of the FREC-II case with the FREC rods down. The difference between the FREC rods up case to the FREC rods down, for the nominal FREC-II is about 15%.

FREC-II was originally designed to provide a large cavity for performing radiation tests, a short pulse width with lower total fluence, and a capability to have radial flux shaping. Figures 14 and 15 show the 89 and 640 neutron energy group flux for both the ACRR central cavity and for the FREC-II cavity. Notice that, for the ACRR cavity, the thermal neutron flux (~10^{-7} MeV) is much smaller than for the FREC-II cavity. For the ACRR cavity, the thermal flux is about 10% of the total flux; for the FREC-II cavity, the thermal flux is about 30% of the total flux. The total neutron flux in the FREC-II is ~13% of the flux in the ACRR cavity.

Table 1. Neutronic Metrics.

Metric	FREC-II FREC Rods Up	FREC-II FREC Rods Down	11.9 in. MITL Port FR UP	11.9 in. MITL Port FR DN	10.2 in. MITL Port FR UP	10.2 in. MITL Port No Fuel
Keff/ Δ Reactivity ($)	1.0253 0.00	1.0234 -0.25	1.0229 -0.31	1.0226 -0.35	1.0231 -0.28	1.0196 -0.74
Neutron Lifetime (μsec)	27.1	25.3	25.2	24.8	25.4	23.9
1-MeV DES Neutron Fluence ($n/cm^2/MJ$)	9.31E11	8.07E11	7.35E11	7.21E11	7.58E11	4.27E11
Total Neutron Fluence ($n/cm^2/MJ$)	2.66E12	2.33E12	2.16E12	2.11E12	2.23E12	1.45E12
Prompt Gamma Dose (krad (Si)/MJ)	1.16	1.01	0.95	0.93	0.98	0.69

Figures 16 and 17 show the neutron and gamma-ray energy spectra at the tally sphere in the FREC-II cavity for the six cases analyzed. For the neutron energy spectra, the results are all very similar, except for the case without fuel. For that case, there is a significant decrease in the fast and epithermal flux. For all of the other cases, there is not very much difference in the spectra. The nominal case with the FREC rods up is larger in magnitude, as expected. The gamma-ray spectra are also very close, except for the case without fuel.

Figures 18 and 19 show the total neutron flux profile through the center of the reactor and cavities. Figure 18 is shown for the whole ACRR/FREC-II reactor, and Figure 19 for the FREC-II cavity. For the nominal case with the FREC rods up, the flux in the ACRR is less because the worth of the FREC-II is larger and contributes more to the total neutron flux and fission power. With the FREC rods up, 33.5% of the fissions occur in the FREC fuel. With the FREC rods down, 13.9% of the fission occur in the FREC fuel. The neutron flux profile can be seen in more detail in Figure 19. The cases analyzed are all very close in value. Only the FREC rods up case and the case without fuel are significant outliers.

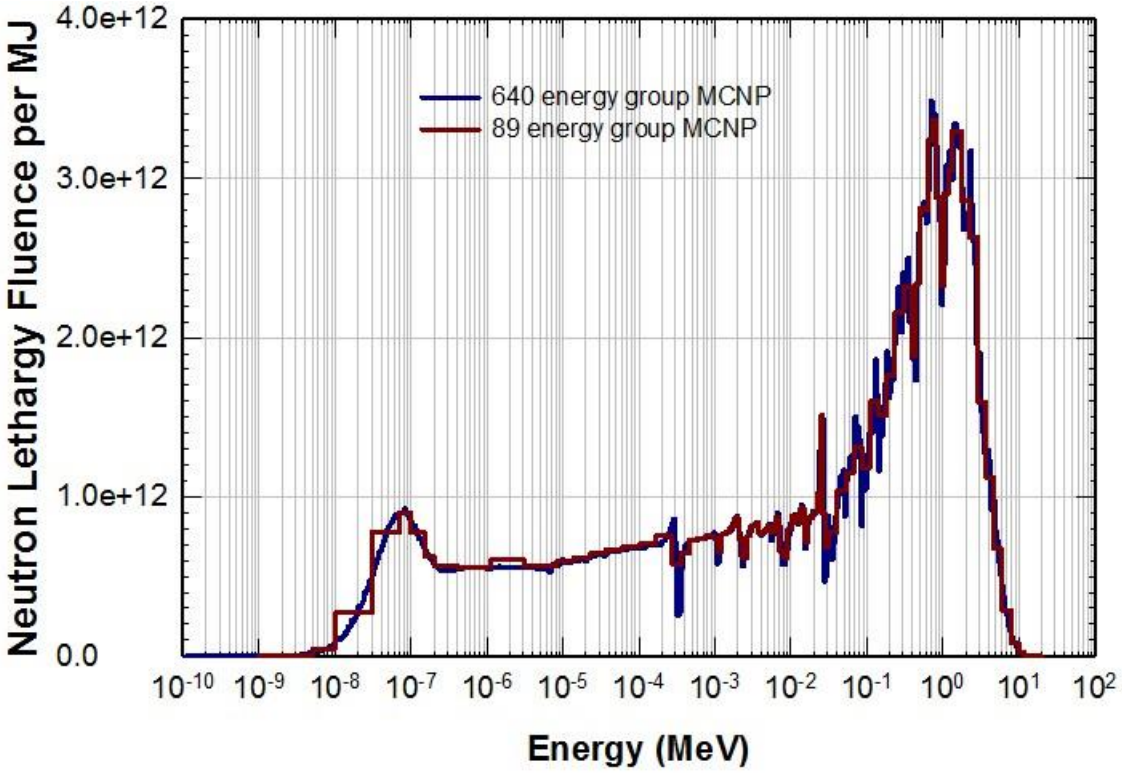

Figure 14. Neutron Energy Spectrum in the ACRR Cavity.

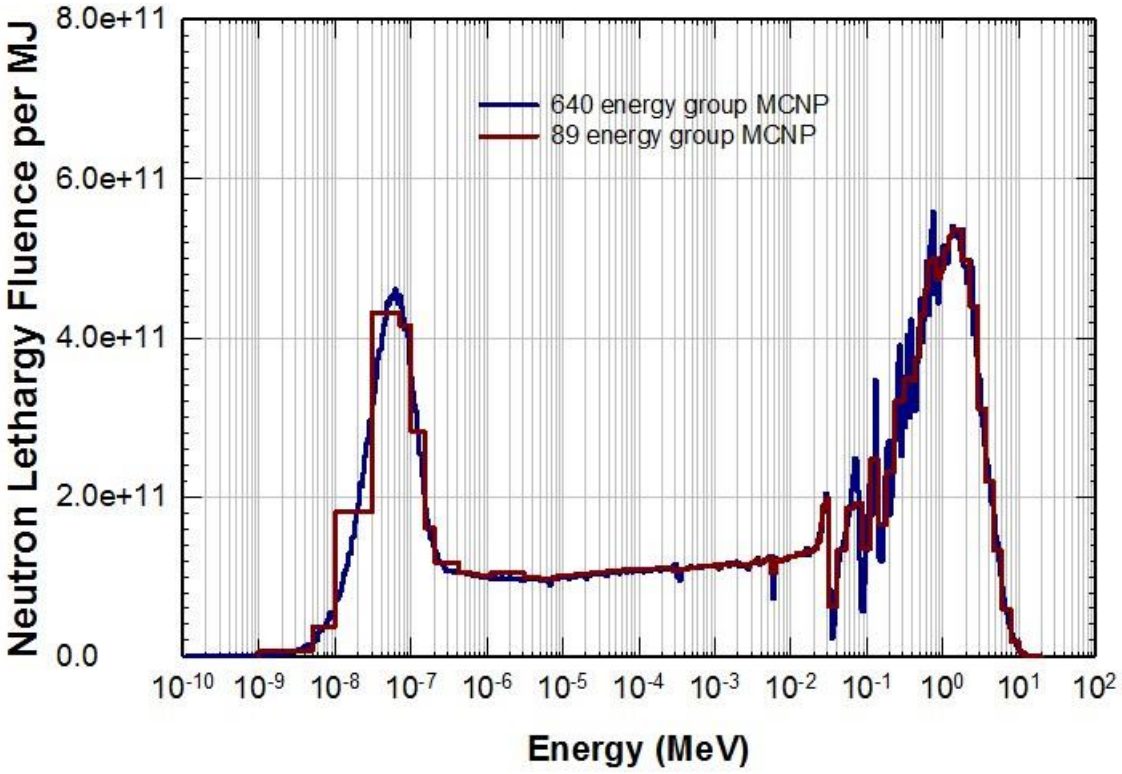

Figure 15. Neutron Energy Spectrum in the FREC-II Cavity.

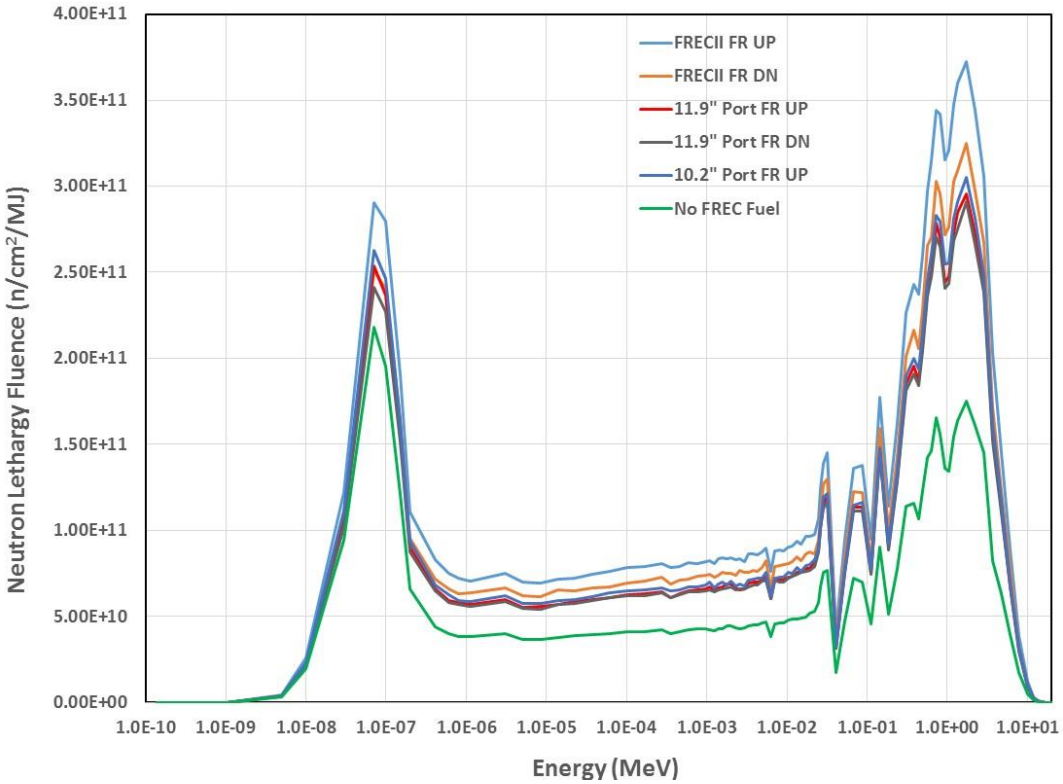

Figure 16. Neutron Energy Spectra for the MCNP Cases Analyzed.

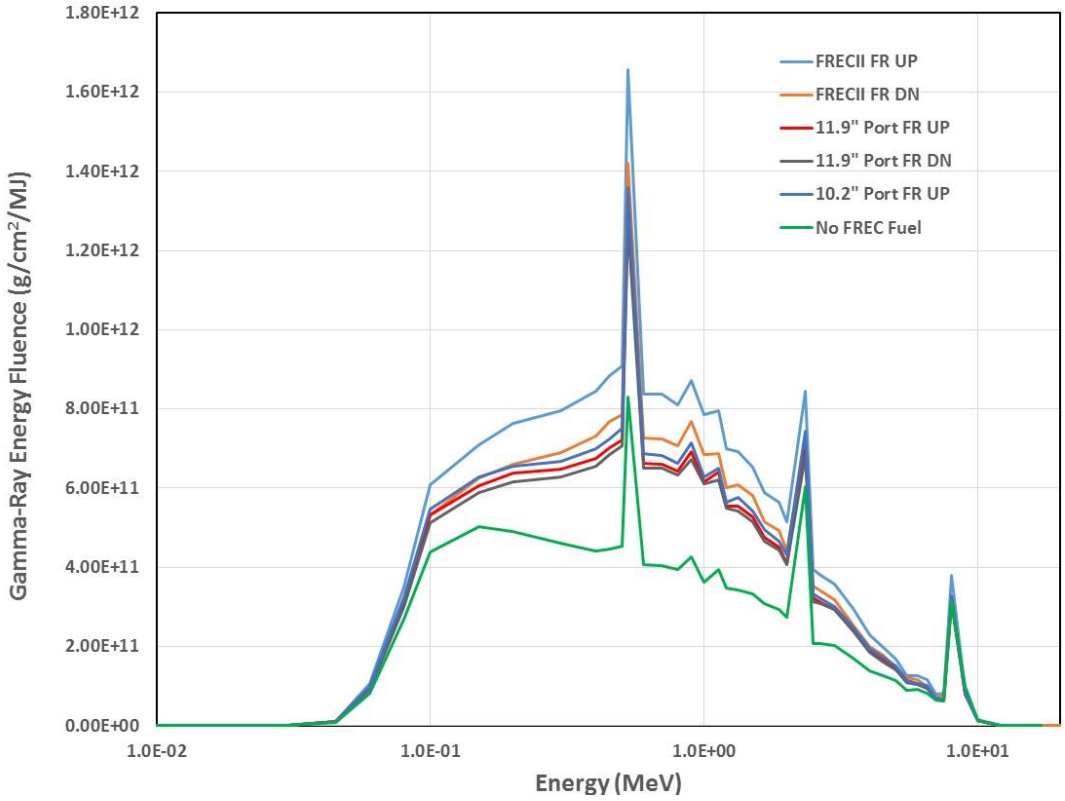

Figure 17. Gamma-Ray Energy Spectra for the MCNP Cases Analyzed.

Most recently, experiment customers using the FREC-II have desired pulses with the FREC rods in the down position, in order to have a larger gradient at the center of the cavity. But as seen in all of the cases analyzed here, there is a strong front-to-back gradient in the flux profile in the FREC-II cavity, even for the nominal case with the FREC rod up. The gradient is more steeped near the front of the cavity at the ACRR interface, and almost constant near the rear of the cavity. Results presented in Ref. 2 show that the thermal flux is relatively constant across the cavity. The epithermal/fast flux maintains shapes very similar to those seen in Figure 19. Most experimenters also desire the epithermal/fast flux as compared to the thermal flux. In many experiments, boron loaded materials or cadmium sheets will be used to remove the thermal neutrons from the flux spectrum. Also, a cadmium-polyethylene bucket and a lead-boron bucket exist for use in FREC-II, that will remove thermal neutrons from the irradiation region. As with any experiment in the ACRR or FREC-II, detailed MCNP modeling of the experiment in the configuration that will be tested must be performed in order to understand the effects on the reactor and the radiation transport in the experiment.

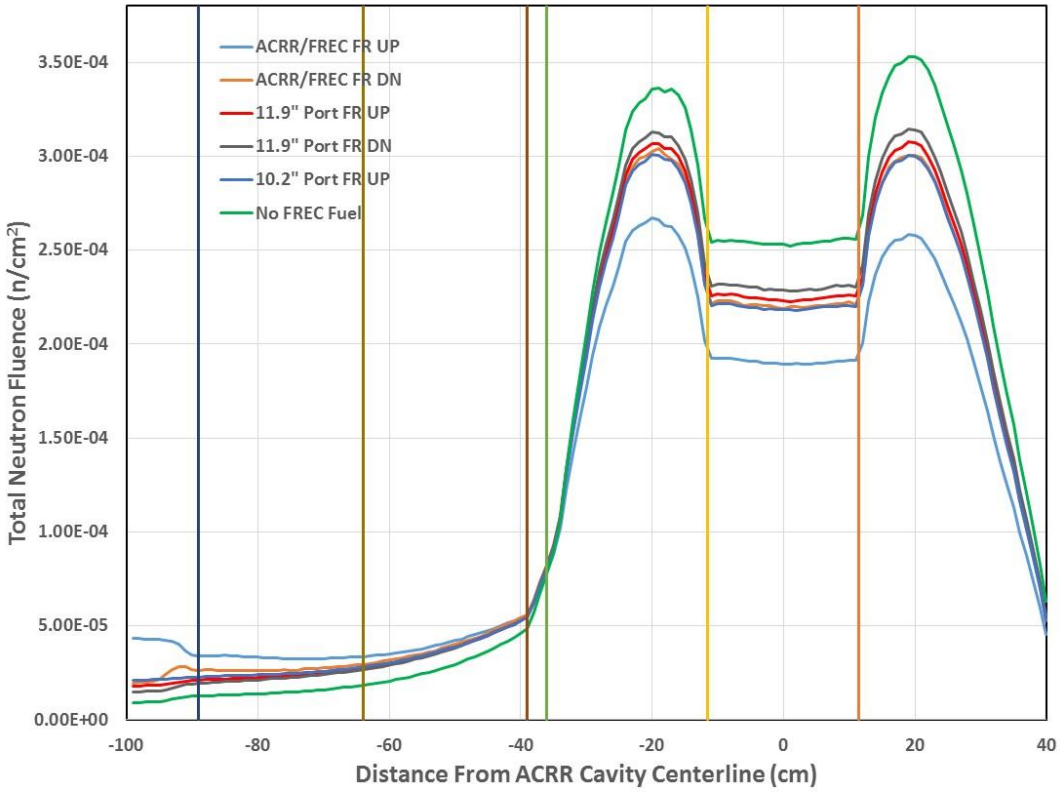

Figure 18. Total Neutron Fluence Radial Profile Through the ACRR and FREC-II for the MCNP Cases Analyzed.

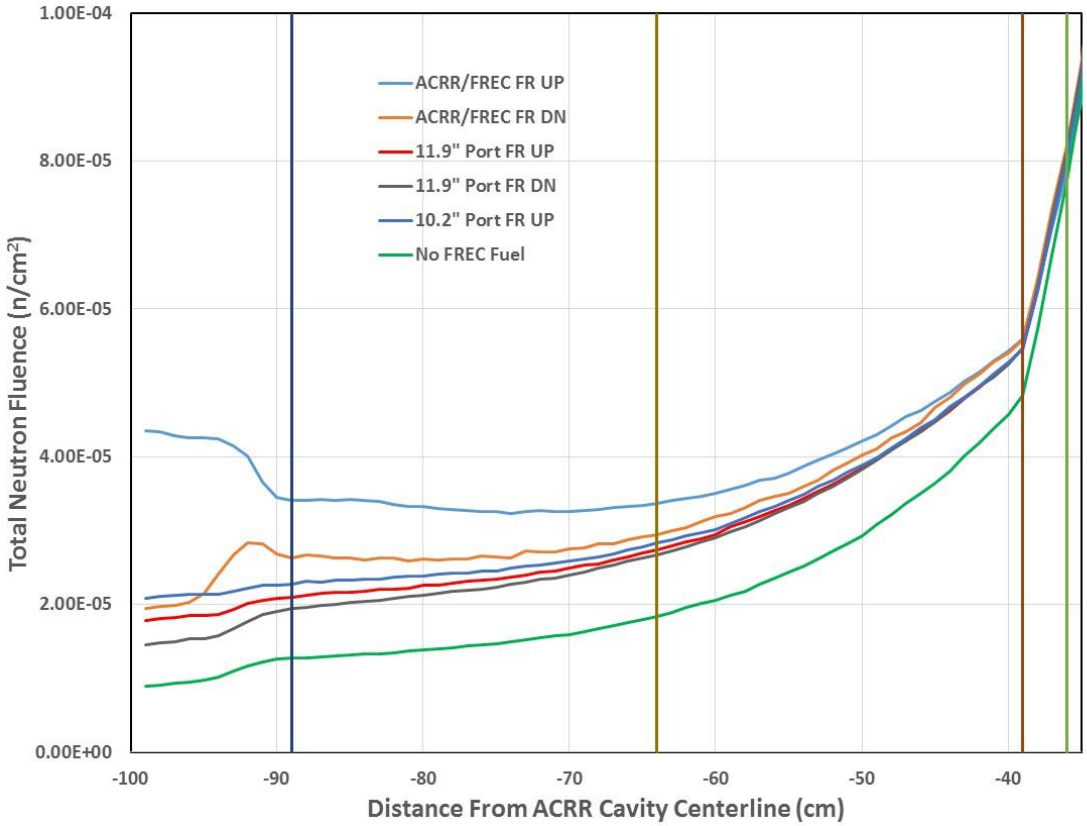

Figure 19. Total Neutron Fluence Radial Profile Through the FREC Cavity for the MCNP Cases Analyzed.

8. Issues

The issues that are of most concern that need additional analyses are as follows:

- EMP effects on ACRR electronics and control system during the accelerator operations;
- Radiation dose and activation from streaming from MITL/MITL port during accelerator operations and when the accelerator is not in use;
- Curved vs straight MITL possibilities to reduce streaming effects;
- MITL/MITL port interfacing with ACRR tank, and FREC-II;
- Movable vs. fixed ACRR/FREC-II for a new facility;
- Safety basis for a combined facility;
- Coupling efficiency of the accelerator to the experiment;
- Cost of the accelerator and interface to the ACRR tank;
- TRL of LTD driver technology and ability meet the capabilities of HERMES-III.

9. Conclusions

The concept of integrating a HERMES-III type pulsed-power accelerator with the ACRR FREC-II cavity is feasible in a new facility. Although a number of issues exist, the basic concept is possible and would provide a capability that currently does not exist in the radiation testing complex. As far as the neutronic characteristic of operating the ACRR and the current experiment capabilities of the FREC-II, no loss in the machine's competences would be realized.

10. References

1. E. J. Parma, G. E. Naranjo, R. M. Vega, L. L. Lippert, D. W. Vehar, P. J. Griffin, "Radiation Characterization Summary: ACRR Central Cavity Free-Field Environment with the 32-Inch Pedestal at the Core Centerline (ACRR-FF-CC-32-cl)," Technical Report SAND2015-6483 (2015)

2. E. J. Parma, G. E. Naranjo, L. L. Lippert. R. D. Clovis, L. E. Martin, K. I. Kaiser, J. Emmer, J. Greenburg, J. O. Klien, T. J. Quirk, D. W. Vehar, and P. J. Griffin, "Radiation Characterization Summary: ACRR-FRECII Cavity Free-Field Environment at the Core Centerline (ACRR-FRECII-FF-cl)," Technical Report SAND2017-8674 (2017)

3. D. B. Sinars, M. E. Cuneo, D. G. Flicker, H. Hanshaw, G. S. Heffelfinger, M. Herrmann, R. M. Hertweck, B. M. Jones, J. Lee, R. W. Lemke, L. Lorence, T. Mattsson, M. K. Matzen, C. Nakhleh, E. J. Parma, Jr., K. O. Reil, V. Harper-Slaboszewicz, W. A. Stygar, "Short-Pulse Accelerator and Reactor Center (SPARC)", SNL Proposal (2012)

A Appendix – Pulsed Power Options – Current and Next Generation Architecture for Linear and Radially Symmetric Accelerators

Current Architecture

A portion of the following section was taken from Sinars, et al, 2012 (Ref. 3). This work was the final report of an investigation in proposing a new Z facility (SPARC-Z) and an externally-driven nuclear assembly (SPARC-Z).

The high-energy density science community has developed many high-current pulsed power accelerators during the past 50 years, where high current means the accelerator delivers >1,000,000 Amperes (1 MA) to a physics target load. The prime-power source of a conventional high-current machine consists of one or more Marx generators. A Marx generator is an array of N capacitors that are charged in parallel to the same voltage (V), and discharged using switches as a stack with a total voltage N*V. Shown in Figure 20, the refurbished Z machine at Sandia is the world's largest and most powerful conventional pulsed-power accelerator. It includes 36 pulsed power modules. The prime power source for each module is a Marx generator. The energy from each Marx generator is passed through four stages of pulse compression before it reaches the target load at the center of the machine. These stages compress the energy in both space and time and increase the energy density (equivalent to pressure) of the electrical power from $2x10^5$ J/m^3 ($2x10^{-6}$ Mbar) to of order 10^{13} J/m^3 (100 Mbar). This large pressure is used to drive experiments to high energy density conditions (>1 Mbar).

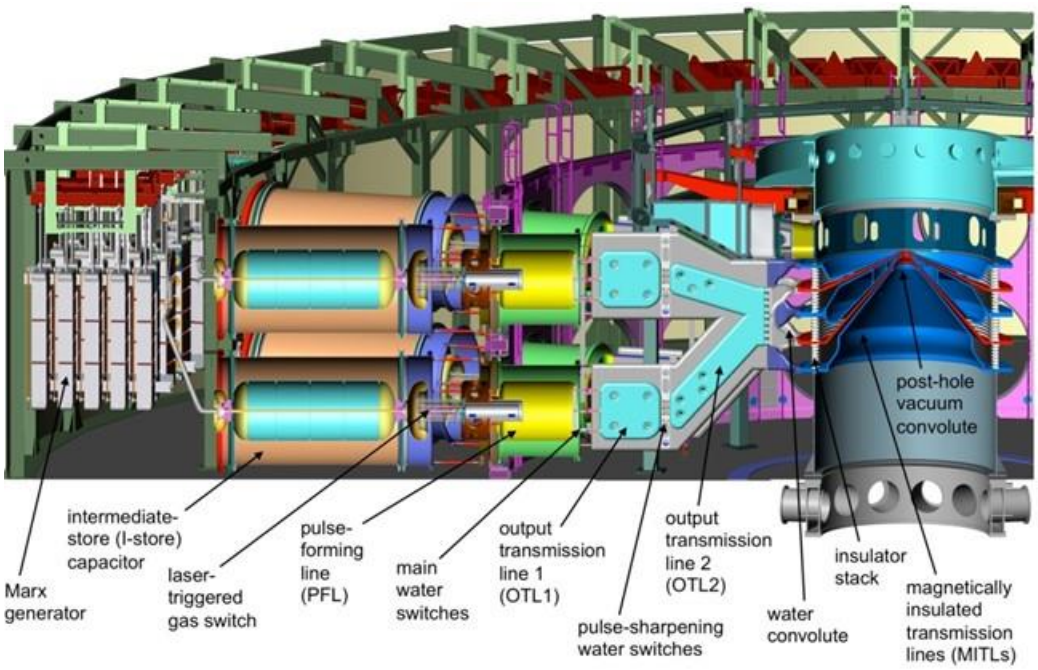

Figure 20. Cross-sectional view of the refurbished Z accelerator showing the various stages of pulse compression.

A Marx generator can be thought of as an LC (inductance/capacitance) circuit; the characteristic discharge time of the current pulse produced by such a circuit is approximately $2(LC)^{1/2}$. The width of the current pulse produced by a Z Marx is 1.5 μs. Experiments conducted on Z require that a linear combination of 130-ns-wide current pulses, one generated by each of Z's 36 modules, be delivered to the load. To produce a 130-ns pulse, each module uses four stages of pulse compression to shorten the pulse produced by its Marx generator. The pulse-compression hardware includes four pulse-forming transmission lines, a laser-triggered gas switch, and two sets of self-closing water switches. To achieve the highest peak currents, the 36 modules are triggered simultaneously so that their energy is combined into a single, 130-ns-wide current pulse. For shockless dynamic materials experiments, the discharges from each of the 36 modules are staggered in time to produce a specific current pulse shape that increases the drive pressure on the sample without creating a shock in the material. Creating the exact current pulse shape needed for each experiment requires precise timing of each module, achieved through a combination of two independent Marx trigger systems and 36 independently timed, laser-triggered gas switches. In this way, current pulses approximately 1 μs in duration have been produced to support experiments.

The pulse-compression stages decrease the efficiency of the accelerator. The stages also increase the effort required to maintain the machine, and make it more difficult to perform an accurate and predictive circuit simulation of an accelerator shot. The design of Z also includes a number of impedance mismatches, which create reflections of the power pulse within the accelerator. Such internal reflections also decrease accelerator efficiency. In addition, they damage the accelerator (after the primary power pulse has been delivered to the load), and make it more challenging to simulate an accelerator shot. For these reasons, scaling this conventional accelerator architecture to higher current and/or voltage levels is not the optimum path forward.

Future Architecture

Future linear and radially symmetric accelerators will be based on a next-generation architecture that improves upon the existing conventional pulsed-power accelerators. While a number of architectures have been proposed for the design of future high-current pulsed power accelerators it is believed by Sandia pulsed-power engineers, that the most attractive approach is based on the Linear Transformer Driver (LTD) architecture. This architecture uses two simple design concepts: single-stage pulse compression and impedance matching.

An LTD can be described as an LC circuit. In conventional pulsed-power accelerators, the characteristic discharge time for the Marx generators are long (e.g., 1.5 μs in the case of Z). Shorter pulses are obtained through multiple pulse compression stages. In the proposed LTD architecture, the time constant is about 130 ns, so *no additional pulse compression stages are needed*. This approach eliminates the inefficiencies and most of the other difficulties that are associated with the pulse-compression stages typically employed by conventional pulsed power machines. The smaller LC time constant is obtained by reducing both the inductance (L) and capacitance (C) of each circuit. The initial energy stored by such a circuit is given by $0.5CV^2$, where V is the initial DC charge voltage. Practical considerations require that the charge voltage be the same as that of a conventional accelerator. Hence to achieve the initial energy storage needed to produce a 60-MA current pulse, the new architecture requires substantially more capacitors than would be needed by a conventional Marx-driven machine.

Example components of the LTD architecture are shown in Figure 21. Prototype LTD cavities composed of capacitors, switches, and magnetic cores are being tested for reproducibility and reliability. LTD cavities have demonstrated reproducible operation on over 12,000 shots at 0.1 Hz, as shown by the example plot overlaying 200 of the current pulses generated during this testing. A high-voltage module can be assembled by yoking multiple cavities together using a central conical conductor. The output voltage of the module is the sum of the voltage across each individual cavity. The capacitors can be grouped in an annular arrangement together with switches and magnetic cores to create a voltage potential across a central gap. This arrangement is referred to as an LTD cavity. The performance of the prototype cavities tested to date is remarkable. The cavities shown can produce about 6 kJ of energy with 70% efficiency and a peak power of 0.05 TW. The timing jitter is 2 ns, with a 0.3% voltage and current reproducibility. Existing switches have demonstrated random failure rates of $<7x10^{-6}$. To obtain higher voltages, multiple LTD cavities can be combined into a larger LTD module as illustrated in Figure 21. An LTD module is essentially a compact induction voltage adder in which each of the adder's induction cavities are driven by capacitors and switches (i.e., LC circuits) that are contained within the cavity. To transport the resulting power pulse to a physics target load, an impedance-matched central conductor is used. This minimizes reflections of the power pulse within the accelerator.

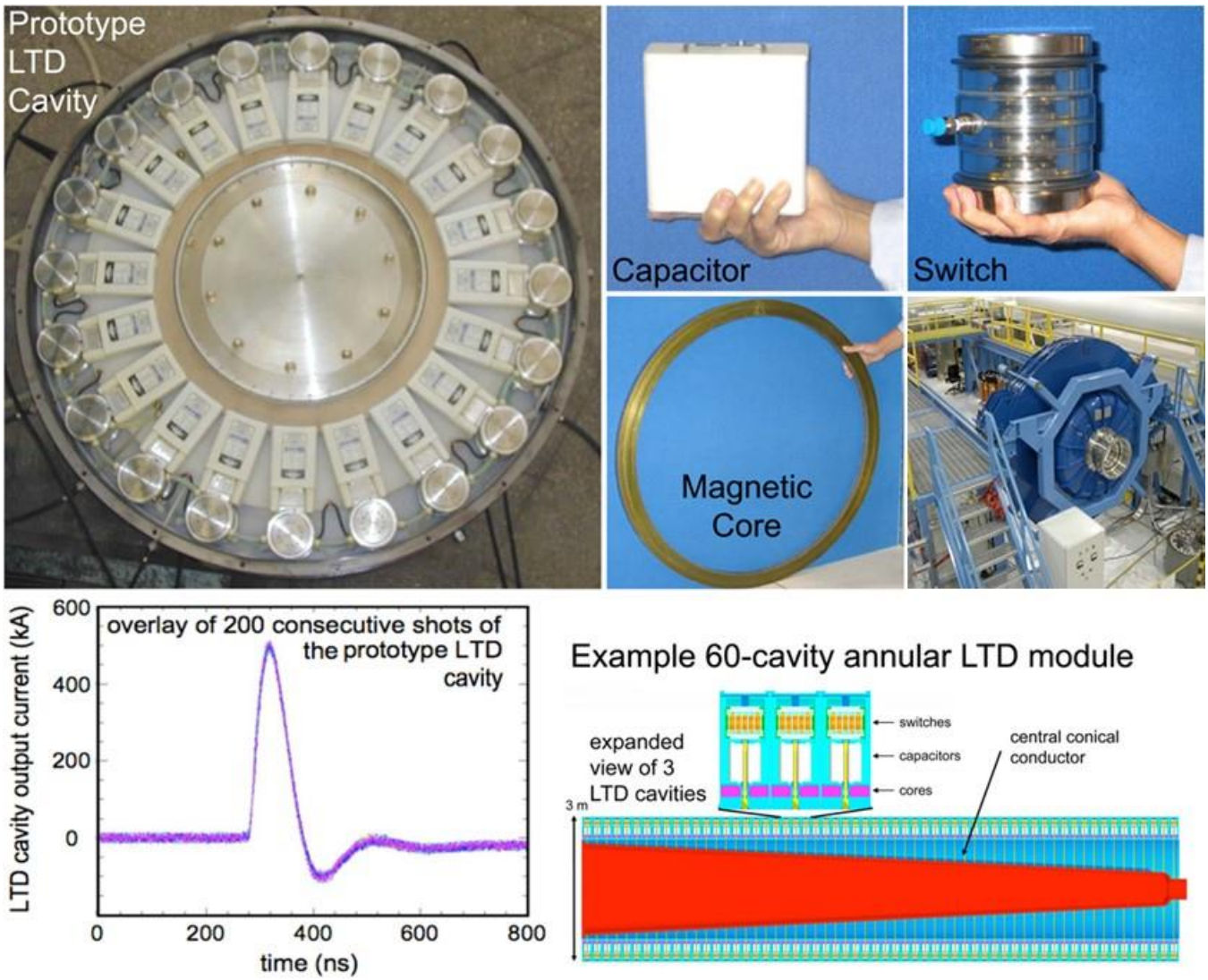

Figure 21. Example Linear Transformer Driver (LTD) technology being tested in the MYKONOS laboratory at Sandia National Laboratories.

Sandia has been evaluating the performance of single LTD cavities for many years. The MYKONOS facility at Sandia, shown in Figure 22, is a multi-cavity LTD module capable of delivering 1 MA of current and up to 1 MV voltage to a target. The facility can ultimately link up to ten 1 MA, 100 kV LTD stages using a common central transmission line to produce this output. The performance of individual cavities and components (e.g., switches) has been improved over the original designs, and further improvements are expected. Tests of the individual cavities and the module as a whole are evaluating the reproducibility and reliability of this unique architecture, which is believed to scale well to the accelerators required to meet both future missions.

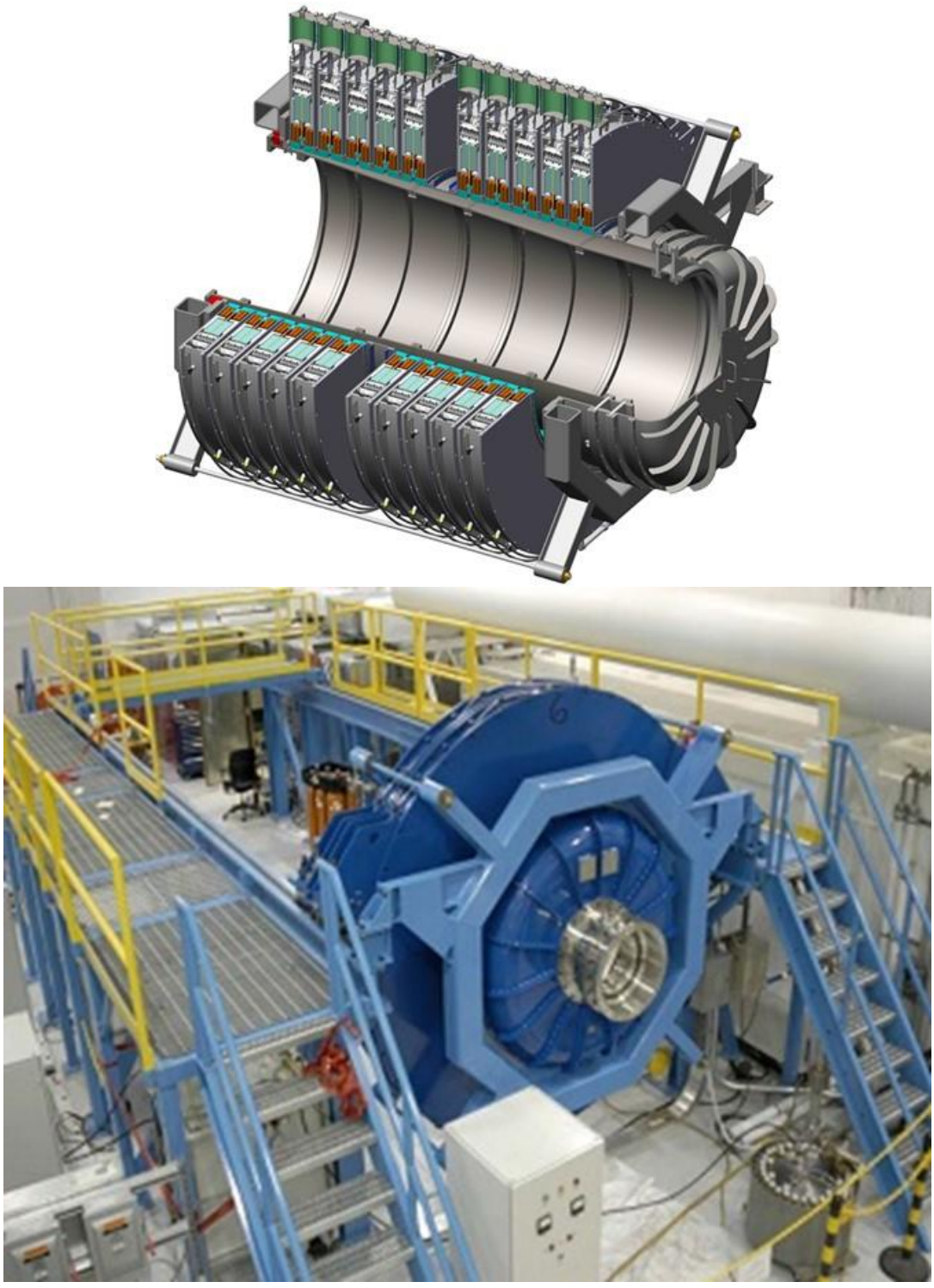

Figure 22. Illustration of the 1 MV, 1 MA MYKONOS pulsed power facility at Sandia.

The LTD-driven accelerator architecture is significantly less complex than that of conventional pulsed power accelerators, since it includes (1) no Marx generators, (2) no intermediate-store capacitors, (3) no megavolt gas switches, (4) no sulfur hexafluoride, (5) no laser-based switch-trigger systems, (6) no pulse-forming transmission lines, (7) no water switches, (8) no magnetic switches, (9) no polarity-reversing cross-over networks, (10) no transit-time-isolated voltage adders, (11) no water convolute, (12) no long self-limited MITLs, (13) no opening switches, (14) no magnetically insulated current amplifiers (MICAs), and (15) no inverse diodes.

Conceptual design for a linear LTD high-current accelerator

Using the architecture illustrated in Figure 21 and 22, a conceptual design was developed for an LTD-based electron beam accelerator called SPARC-E. A total of 560 0.15-TW LTD cavities would be yoked together with a center conductor in vacuum to produce an 84-TW, 56 MV, 1.5 MA electron beam with a characteristic discharge time of about 170 ns. The energy-storage capacity of the accelerator would be about 13 MJ. The width of a single LTD cavity is about 0.2 m. If the cavities were stacked along a single line, the total length would be over 120 m. The conversion efficiency of electrical energy into the electron beam would be about 75%. The SPARC-E proposal was developed for use to drive a LEU-EDNA target. This design significantly exceeds what would be required for a combined environment test designed to meet the HERMES capabilities. The total length of a system to meet the HERMES III capabilities would be less than 30 m (100 ft) in length. This length would be about twice that of the existing HERMES III. However, the diameter of the LTD systems would be about 1/10 that of HERMES III. The SPARC-E accelerator is an inductive-voltage adder MITL. MITL-inductive-voltage adders have been in operation for more than 20 years; Sandia's HERMES III inductive-adder operates at 18 MeV and 750 kA, and utilizes 20 inductive cavities of older design. HERMES III has efficiently propagated current for up to 30 meters along a transmission line. The physics basis for voltage adders and long MITLs is therefore very mature. The SPARC-E accelerator is a factor of 50% scale up in current and 3.1 scale up in voltage, but is based on the more compact, lower cost, inductive cavity architecture of the LTD.

Distribution

1	MS1169	Charles Barbour, 1300 (electronic copy)
1	MS1142	Matt Burger, 1380 (electronic copy)
1	MS1146	Ken Reil, 1384 (electronic copy)
1	MS1146	Pat Griffin, 1340 (electronic copy)
20	MS1146	Ed Parma, 1384
1	MS0899	Technical Library, 9536 (electronic copy)


Sandia National Laboratories